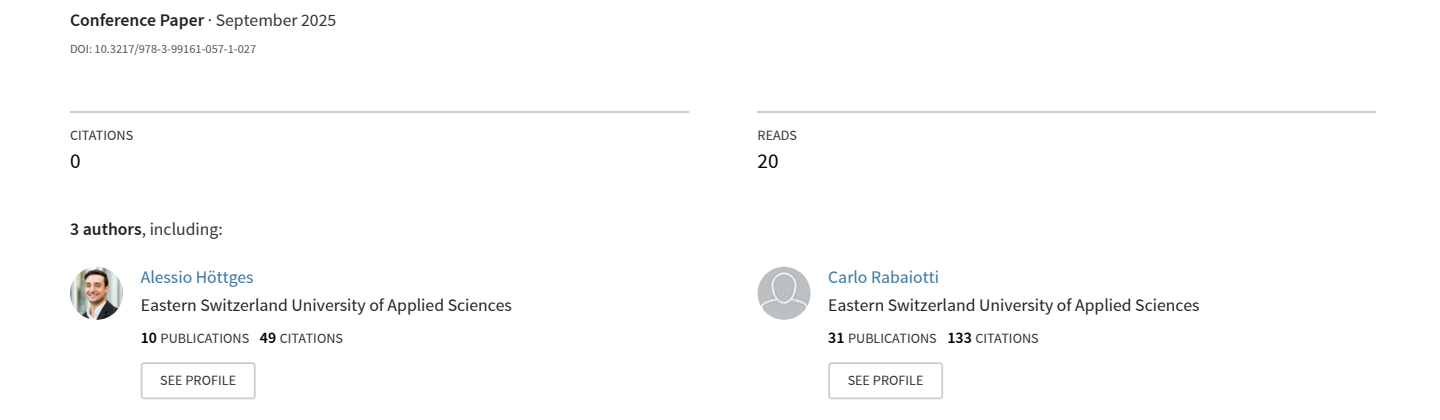
Fibradike sensor: validation through full-scale field testing





Fibradike sensor: validation through full-scale field testing

A. Höttges^{1,2,0000-0003-0315-2563}, C. Rabaiotti^{1,0000-0002-6217-5848}, A. Rosso³

¹Institute for Building and Environment (IBU), Dept. of Architecture, Building, Landscape and Space (ABLR), Eastern University of Applied Sciences (OST), Oberseestrasse 10, 8640 Rapperswil, Switzerland ²Laboratory of Hydraulics, Hydrology and Glaciology (VAW), Dept. of Civil Environmental and Geomatic Engineering (D-BAUG), Swiss Federal Institute of Technology in Zurich (ETHZ), Rämistrasse 101, 8092 Zurich, Switzerland ³Interregional Agency for the Po River, Strada Giuseppe Garibaldi 75, 43121 Parma, Italy

email: alessio.hoettges@ost.ch/alessioh@student.ethz.ch, carlo.rabaiotti@ost.ch, alessandro.rosso@agenziapo.it

ABSTRACT: Earthen geohydraulic structures, such as dams and river embankments, are vital for water resource management and flood control, especially as climate change and urbanization increase hydrological risks. Internal erosion, often triggered by seepage, remains a major failure mechanism and can cause sudden, catastrophic collapses. Traditional monitoring systems lack the spatial and temporal resolution needed for effective early detection. To address this gap, a novel Distributed Pressure Sensor (DPS) based on distributed fiber optic (DFO) technology has been developed by the University of Applied Sciences of Eastern Switzerland (OST). The DPS offers high spatial resolution and extended range, enabling precise measurement of distributed pore water pressure - key for early detection of internal erosion processes. Following successful laboratory validation, the DPS was deployed in a full-scale test embankment (84 m long, 39 m wide, 4 m high) at the AIPo Research and Technical Centre in Boretto, Italy. Preliminary results show that the DPS accurately captured pore pressure evolution, matching conventional piezometer readings while detecting localized variations and two-dimensional flow effects that point sensors could not resolve. These findings highlight the DPS system's strong potential for improving early warning capabilities in geohydraulic structure monitoring.

KEY WORDS: Dike Monitoring, Distributed Pressure Sensor, Distributed Fiber Optic technology.

1 INTRODUCTION

River dikes and earthen dams play a crucial role in water management, including energy production and flood risk protection. Following the catastrophic events in northern Italy of May 2023 [1] and the Rhone region of Switzerland in June 2024 [2], the need for enhanced protection and monitoring of such structures has become evident.

The primary failure mechanisms of these structures are overtopping and internal erosion [3]. Among them, internal erosion is often underestimated and typically not clearly detectable after failure [4].

Conventional monitoring systems, which rely mainly on point-based sensors, are limited in both spatial and temporal resolution. As a result, monitoring during flood events often still depends on visual inspections, sometimes involving hundreds of volunteers, which reflects an outdated approach [4].

In last decades, a promising monitoring alternative has emerged: the use of Distributed Fiber Optic (DFO) technology, which enables high-resolution measurements of temperature and deformation along the entire length of the installed sensing cable [5]-[6]. In this context, an innovative development within the DFO sensor family has been proposed by Höttges, et al. [7], who introduced a Distributed Pressure Sensor (DPS). This sensor is capable of measuring pore pressure with high sensitivity and accuracy, over distances of several kilometers. The DPS is designed to monitor seepage anomalies by directly measuring pore pressure within the structure, which can serve as an early indicator of internal erosion processes as pointed out by Fell, et al. [4].

The DPS has already been validated through extensive laboratory testing on model dikes (Höttges, et al. [7]; Höttges, et al. [8]). This paper presents a further step in the validation

process of this novel sensor by reporting preliminary results obtained under full-scale field conditions, using a dedicated full-scale test embankment constructed at the AIPo Research and Technical Centre. The objective is to assess both the installation process and the sensor's performance in a controlled field environment that closely replicates field operating conditions.

2 DISTRIBUTED PRESSURE SENSOR - DPS

The sensor was developed within the framework of the FIBRADIKE project [9], whose core objective was the development of a DPS based on DFO technology. The sensor, whose latest design has a diameter of 13 mm, consists of an optical fiber that is wound helically around a cylindrical, compressible central element (Figure 1). When the central element is subjected to hydrostatic pressure, it compresses, causing the helical fiber to deform accordingly. The hydrostatic pressure is then back calculated using a calibration coefficient (C_P) that converts the measured radial strain of the fiber into corresponding pressure values. This coefficient is determined by laboratory testing under controlled pressure conditions. According to Höttges, et al. [8] the sensor can reach a sensitivity of 100 Pa and an accuracy of 15 % RD (relative deviation of reading) for a spatial resolution in the order of a few centimeters using the Rayleigh interrogation technique [10]. Additionally, the core of the central element is equipped with two single-mode fibers and two multi-mode fibers, loosely housed in a central tube (see Figure 1), which can be used for Distributed Temperature Sensing (DTS). This configuration enables simultaneous monitoring of pore pressure and temperature, enhancing the sensor's capability for detecting and characterizing seepage-related anomalies. Additionally, the inner part of the central element is filled with aramid yarns (see

Figure 1), which according to Höttges, et al. [8], can provide a tensile strength of up to 20 kN. This feature is particularly useful for installations requiring high tensile strength of the cable, such as pulling or trenching operations.

The sensor was developed and calibrated for pressures up to 200 kPa, specifically designed to operate within the typical pressure range found in river dikes. Although higher pressure ranges are possible, they were not tested in this study. The sensor demonstrates good repeatability and low hysteresis within the tested pressure range [7].

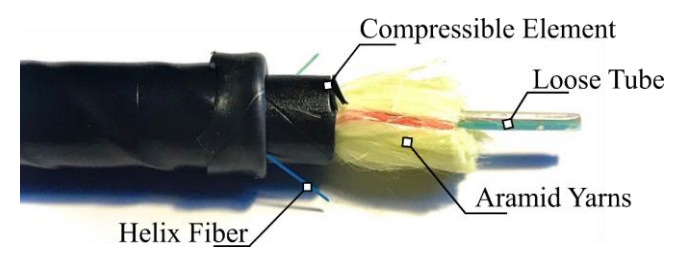


Figure 1. Design of the DPS, adapted from [7].

3 FULL-SCALE TEST EMBANKMENT

3.1 Embankment design and construction

The test embankment is constructed at the AIPo Research and Technical Centre situated in the municipality of Boretto - Province of Reggio Emilia (RE – Italy). The test embankment has a length of 84 m, 39 m wide and 4 m high with a slope 1:2 [9], see Figure 2. The embankment is founded on 16 m thick clay layer and 16 m thick medium to coarse sand (aquifer), from which water is pumped to fill the reservoir.

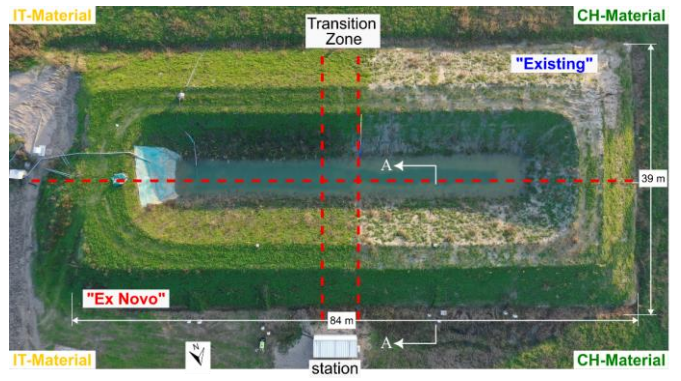


Figure 2. Test embankment with the 4 different sections.

The test embankment was constructed using two different materials: a coarse soil typical of Swiss river dikes and a finer soil characteristic of the river dikes along the Po River plain. These two zones are referred to as Swiss (CH) and Italian (IT) sections, respectively. According to the Unified Soil Classification System (USCS), the IT-Material is classified as sandy clay (CM), while the CH-Material is classified as clayey sand (SC). The granulometric distribution of the two materials is shown in Figure 3. Based on in-situ permeability tests, the permeability k_m is approximately $1 \cdot 10^{-5}$ m/s for the CH and $2 \cdot 10^{-7}$ m/s for the IT-Material.

Two different sensor installation methods were also implemented, each applied to a different section. The first, referred to as "ex novo", simulates the sensor installation during the construction process. The second, referred to as "existing",

involves the installation of the sensors after the construction of the basin has been completed, using the Horizontal Directional Drilling (HDD) technique [11].

In total, four different zones were constructed, each representing a unique combination of material type and installation method (Figure 2). This paper focuses solely on the installation and results of the "ex novo" section.

The test embankment was constructed using the described two different materials, placed in 30 cm thick compacted layers. Each layer was compacted using a roller compactor (about 6 passes per layer) with the optimal water content determined in the laboratory. The Swiss section was additionally equipped with a gravel filter, designed to prevent toe erosion failure. To prevent localized seepage inhomogeneities, the transition zone between the two materials (Figure 2) was constructed by interlayering both material types.

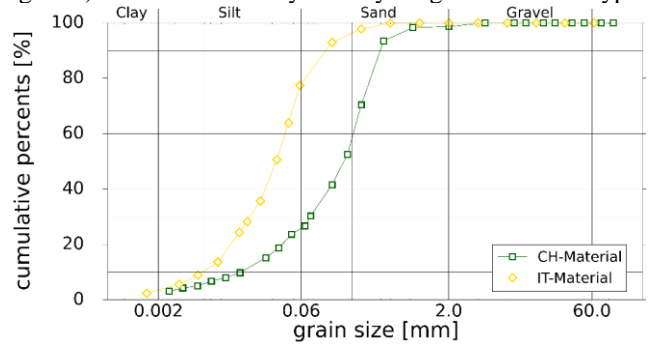


Figure 3. Granulometry of CH-material and IT-material.

3.2 Experimental setup

The DPS sensor was installed in the "ex novo" section during construction, arranged in a mesh pattern at three different elevations (z) from the bottom of the basin: z=0.3 m (Layer 01), z=1.3 m (Layer 02), and z=2.3 m (Layer 03). Figure 4 illustrates the DPS cable mesh installed in Layer 01, showing two main orientations: the longitudinal (L) direction (x-axis) and the transversal (T) direction (y-axis). The longitudinal direction is defined as parallel to the assumed river flow, while the transversal direction is parallel to the seepage flow within the dike. The DPS was installed in two different configurations: as a free cable, and within saturable tubes (black rectangles in Figure 4) equipped with porous stones. These tubes are designed to protect the DPS from earth pressure variations and to ensure that only hydrostatic pressure is measured in those sections.

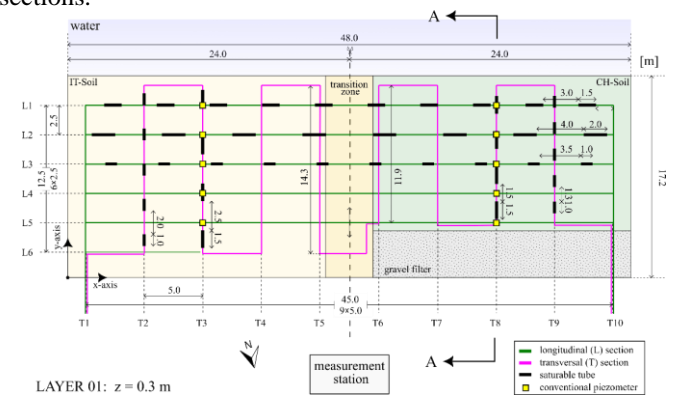


Figure 4. Mesh installation of the DPS in Layer 01 of the "ex novo" section.

To validate the DPS measurements, 10 conventional piezometers were installed in two main cross-sections (T3 and T8) of the "ex novo" section in Layer 01 (indicated by yellow square in Figure 4). The piezometers are of the vibrating wire (VW) type, with a measurement range of 0-170 kPa and an accuracy of $\pm 0.4\%$ of full scale (FS). Figure 5 shows the installation layout of both the DPS sensors and the piezometers along the A–A cross-section indicated in Figure 2.

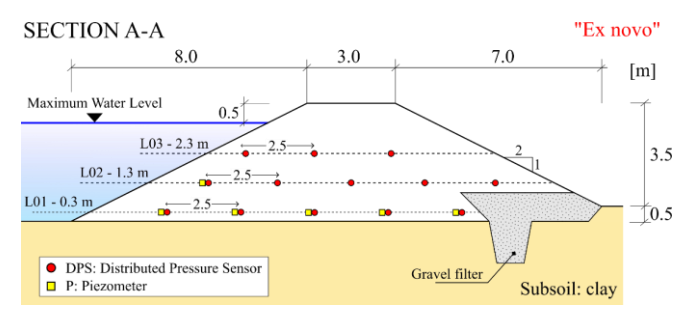


Figure 5. A-A cross section of the installation.

3.3 Testing procedure

The water level values recorded during the test are presented in Figure 6. Initially, the water level stood at 1 meter due to rainfall accumulation and was raised to 2.3 meters by pumping groundwater from the aquifer through an existing well (Phase 1: Filling – about 5 h). After reaching the target level, the basin was allowed to drain naturally for approximately one week (Phase 2: Self-Drain – about 165 h). This was followed by a controlled, three-stage emptying process designed to reduce the risk of instability associated with rapid drawdown (Phase 3: Emptying – about 70 h). The water level was monitored using a piezometer installed at the water-side toe of the test embankment.

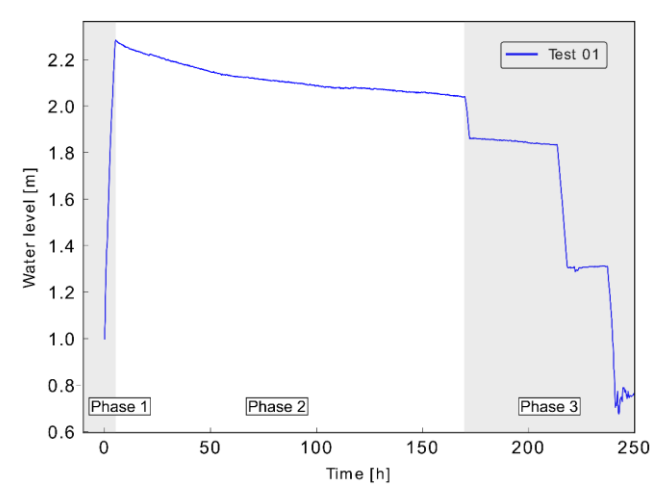


Figure 6. Water level inside the basin during the test.

The data from the DPS helical fiber were collected manually at approximately 30-minute intervals using a commercially available Rayleigh-based Optical Backscatter Reflectometer (OBR 4600, Luna Innovations [12]). Due to the manual acquisition process, measurements were limited to the initial filling Phase 1 and continued for approximately 12 hours of the Phase 2. The core temperature fiber was automatically interrogated using a Raman-based system (AP Sensing, DTS - N45 Series [13]), with an acquisition time of 4 minutes.

Conventional instruments recorded data automatically every 15 minutes. Temperature and piezometer measurements were recorded continuously until the end of the test, when the basin was fully emptied (after approximately 240 hours).

3.4 Data processing

The data obtained from the DPS were post-processed using a spatial sampling interval of 10 cm and a spatial resolution of 10 cm, with a reference that was updated after each measurement. This approach reduces noise that would otherwise accumulate if the initial measurement were used as a fixed reference throughout the test. The spectral shift values were then cumulatively summed after each iteration.

Subsequently, artificial peaks were removed using the "peak prominence" method available in Python [14], which identifies local maxima by comparing each value to its neighboring points. Detected peaks were then replaced with the median value of their surrounding neighbors. The resulting data were then smoothed using a Savitzky-Golay filter [15].

The filtered values obtained were then converted to pressure using the pressure coefficient C_P (described in section 2).

The raw data from the DTS system were not post-processed, as the results provided by the instrument were already corrected through automatic calibration in loop mode. A sampling interval of 1 meter, a spatial resolution of 0.5 meters, and a measurement time of 1 minute were used.

The piezometer data were not corrected, as both barometric and temperature corrections have minimal influence and were therefore neglected.

3.5 Preliminary Results

Figure 7 illustrates the pore pressure measured with piezometers in Layer 01 (Figure 4) for the two different materials at four time intervals: at the start of the test, and after 12, 24, and 60 hours (Figure 6). The corresponding water levels, shown in blue, are also reported in Figure 7, for these intervals.

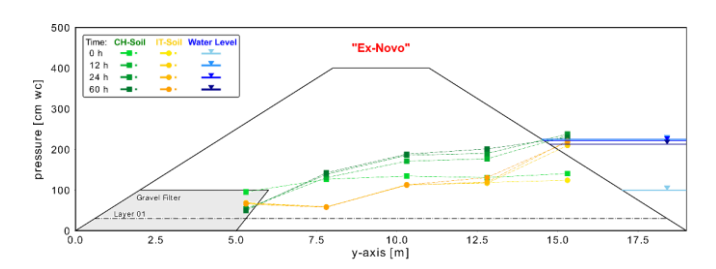


Figure 7. Piezometer measurements for the two soil materials at four time intervals (0h, 12h, 24h and 60 h) in Layer 01.

Figure 8 presents the post-processed pressure variation measurements across all transversal sensor lines from T4 to T9 in Layer 01 (Figure 4) for five different time: 1.6 h, 3.1 h, 4.2 h, and 10.2 h. These results represent the distributed pressure data along the full fiber length (axial cable development), obtained from the DPS system after applying filtering and peak correction techniques, as described in section 3.4. The pressure variation is calculated cumulatively by changing the reference measurement taken from the beginning of the test when the water level in the tank was already 1 m high. The longitudinal segments of the transversal loop are referred to as the "wet

side" (WS) when the segment is on the water-facing side of the embankment, and the "dry side" (DS) when it is on the airfacing side; see Figure 4.

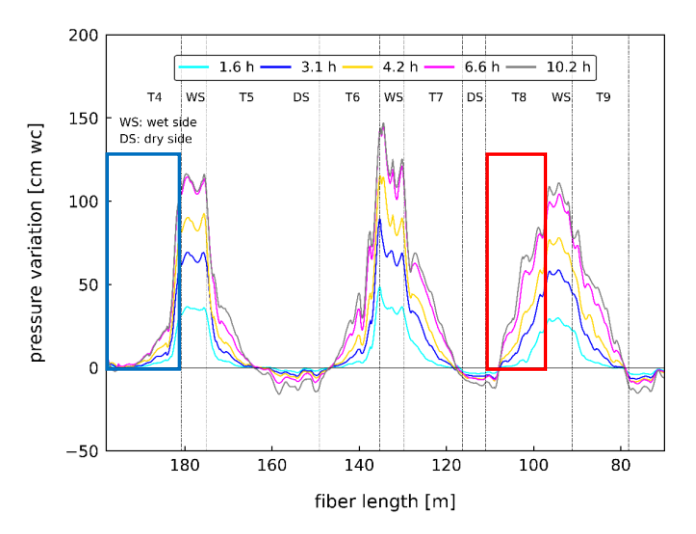
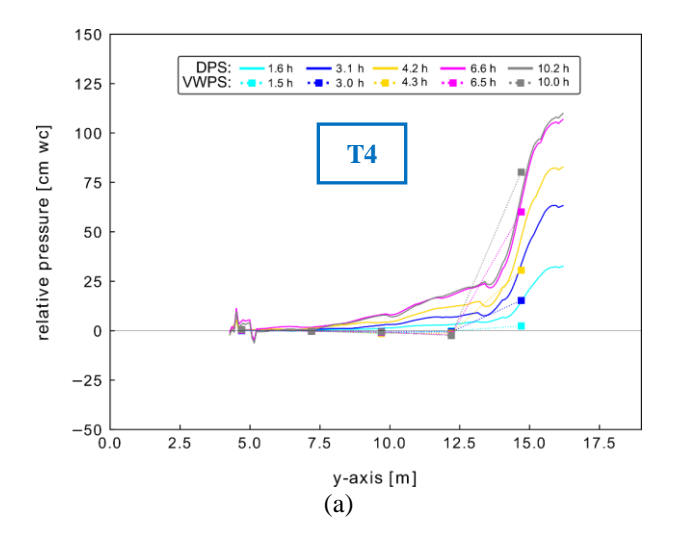


Figure 8. Pressure variation measured during the filling phase using the transversal DPS cables in Layer 01.

It should be noted that the data from lines T2 and T3 exhibited increased noise and irregularities, due to localized issues related to sensor splicer connections during the test. For this reason, these data were excluded from the results analysis.

Figure 9 (a) shows a comparison between the vibrating wire piezometer sensors (VWPS) and the transversal DPS cable measurements at T4 (see Figure 4), while Figure 9 (b) presents the same comparison at location T8. The analysis was conducted at T4, which is also situated within the IT-Material section. Both figures show the results for the same time intervals as shown in Figure 8.



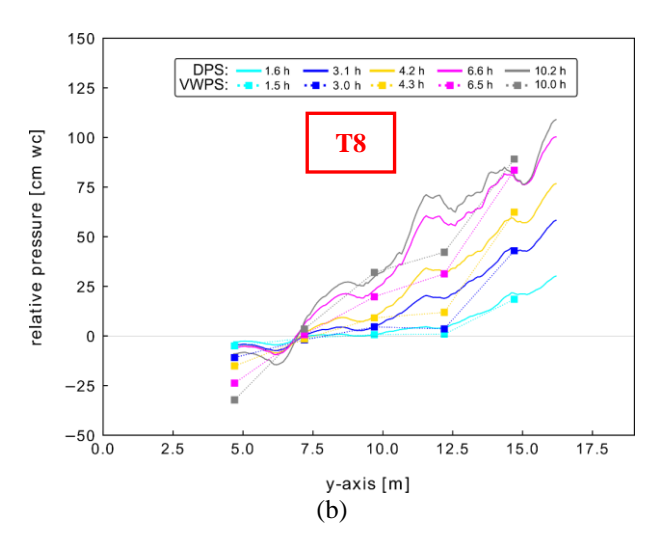
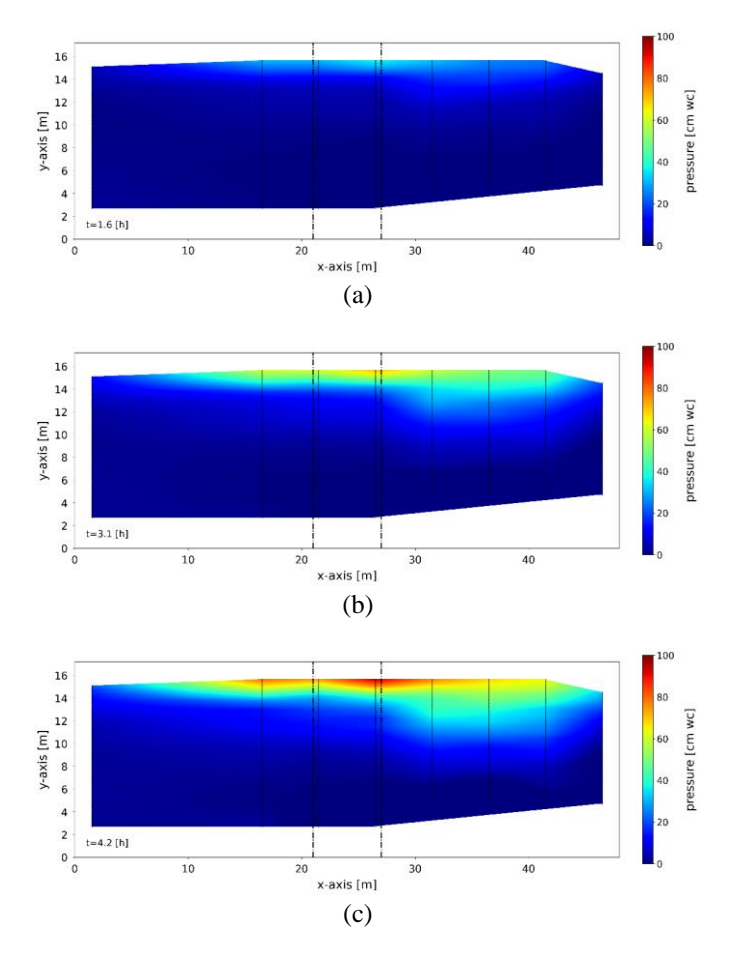


Figure 9. Comparison between the DPS measurements and the vibrating wire piezometer sensors (VWPS) at different time intervals in the transversal direction: (a) T4 and (b) T8.

Figure 10 shows a colormap of Layer 01 based on the transversal DPS measurements presented in Figure 8. The colormap was generated using bicubic interpolation of the transversal DPS data, with additional measurement from T1 and T10, which were obtained from the longitudinal cable L1 (see Figure 4).



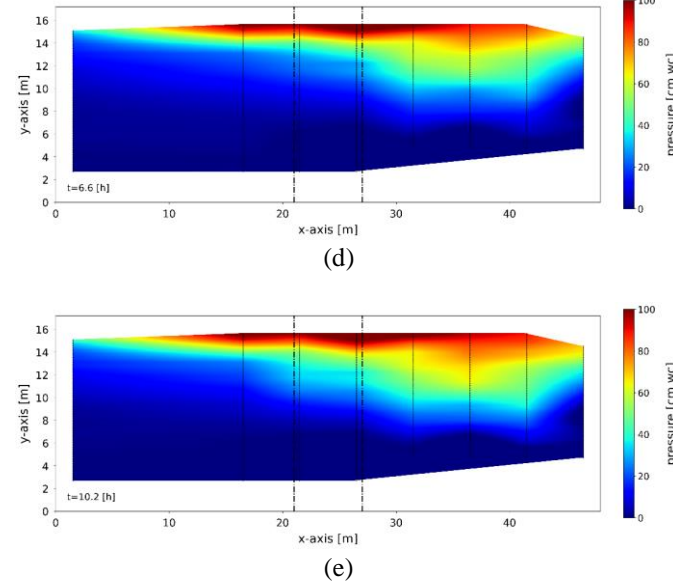
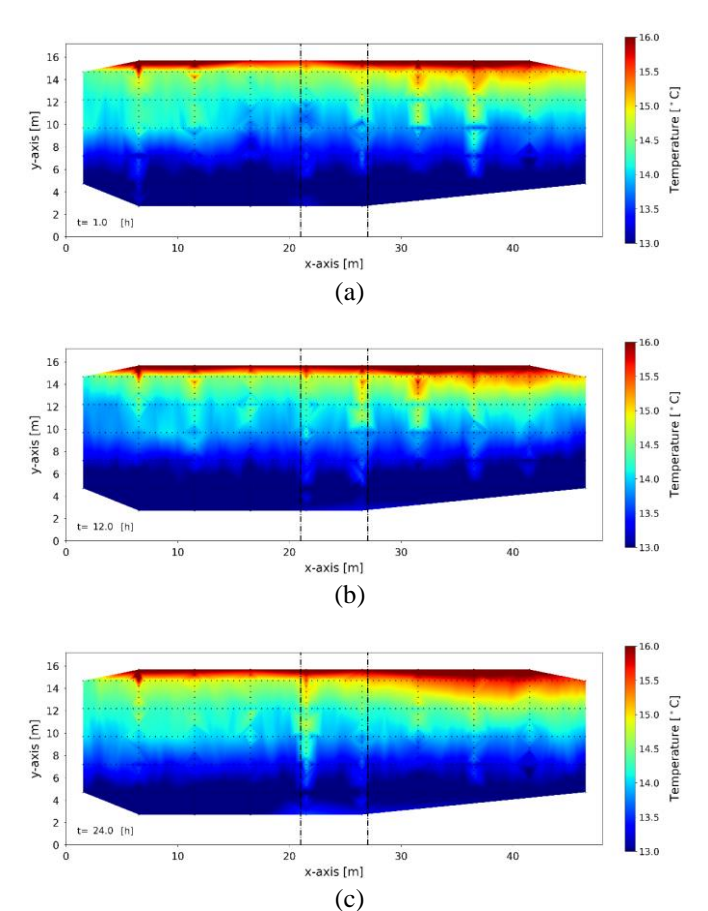


Figure 10. Distributed temperature results for transversal section of Layer 01 at (a) 1.5 h, (b) 3.1 h, (c) 4.2 h, 6.6 h, and (d) 10.2 h after the start of the test.

The absolute temperature distribution obtained by the core temperature fiber of the DPS cable is shown in Figure 11 at four time intervals: 1 hour, 12 hours, 24 hours, and 144 hours after the start of the test. Similar to Figure 10, the data are displayed as colormaps using bicubic interpolation, derived from both the longitudinal and transversal cable sections in Layer 01 (see Figure 4).



CC BY 4.0 https://creativecommons.org/licenses/by/4.0/deed.en This CC license does not apply to third party material and content noted otherwise

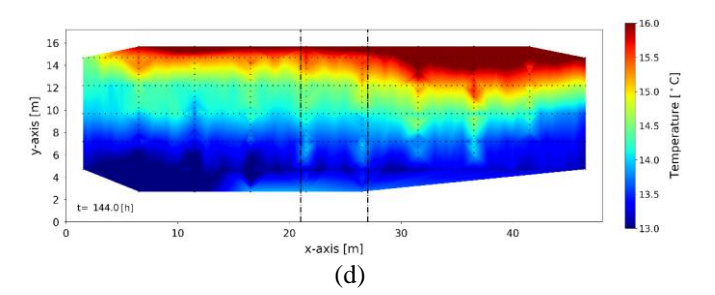


Figure 11. Distributed temperature results for Layer 01 at (a) 1 h, (b) 12 h, (c) 24 h, and (d) 144 h after the start of the test.

4 DISCUSSION

The initial pore pressure measurements (Figure 7) confirmed that the sensors installed in Layer 01 were already below the seepage line prior to the test, consistent with the 1 m water level maintained due to prolonged rainfall.

The Swiss (CH) material, with its coarser granulometry and higher permeability, responded more rapidly to water level changes compared to the IT-Material, which had a finer particle distribution and lower permeability. This contrast is evident in both the vibrating wire piezometer sensor (VWPS) measurements (Figure 7) and the DPS readings (Figure 8 and Figure 9). In particular, the DPS captured a steeper and delayed pressure curve within the IT section, aligning with the expected slower hydraulic response. Additionally, a minor effect from the activation of the drainage filter in the Swiss section is observed, indicated by a slight decrease in pore pressure recorded by the piezometer and the DPS installed at that location.

A good agreement was observed between the VWPSs and the DPS measurements (Figure 9). However, in the central part of the transversal section, the DPS shows slightly higher pore pressure variations compared to the VWPS. When comparing the time intervals, it is evident that the DPS system responds more rapidly than the VWPS particularly during the first interval at 1.5 hours. The DPS captures changes in pore pressure almost instantaneously, whereas the VWPS exhibits a slightly delayed response due to its mechanical components and different response time [16, 17]

The effect of the saturable tube on the DPS cable is particularly noticeable in the CH-Material section, as shown in Figure 9 (b), where a region of constant pore pressure is observed at a distinct location.

Colormap visualization (Figure 10) clearly delineates the transition between the CH and IT materials, demonstrating the DPS's capability to resolve subtle spatial variations in pore pressure distribution. Moreover, the boundaries around sensor lines T1 to T10 exhibit signs of two-dimensional (2D) pore pressure effects within the plane of Layer 01, suggesting more complex flow dynamics in these regions that deviate from the assumed one-dimensional (1D) behavior.

Temperature measurements (Figure 11) remained stable during the first 24 hours. Since the DTS cables were installed below the initial seepage line (see Figure 7), no significant temperature changes were expected during the test period, which is consistent with what was observed. A slight temperature increase was detected only after approximately 144 hours, particularly in the CH section, which is consistent with the higher thermal conductivity expected in coarser soils.



Since the DPS data were collected within the first 17 hours during which temperature variations were negligible - no temperature correction was applied to the pressure data.

Approximately one year after installation and following the test results presented, some localized disturbances or breaks in the sensor signal were observed. These problems were probably caused by small mammals such as mice or beavers - and were related to the reduced mechanical robustness of the earlier DPS cable design, which was installed in the "ex novo" section and featured a thinner outer protective layer. This vulnerability highlighted a practical limitation in field applications. In response, newer DPS cable designs were developed with an enhanced outer protective layer to improve durability and mitigate such risks, thereby increasing long-term reliability in real-world conditions.

5 CONCLUSION AND OUTLOOK

The application of a novel Distributed Pressure Sensor (DPS) system was evaluated through field testing on a full-scale test embankment at the Research and Technical Centre of the Agency for the Po River (AIPo) in Boretto, Italy. Preliminary results, supported by comparisons with traditional piezometer measurements, confirm that the DPS system can be effectively deployed as a distributed pore pressure sensor. In contrast to point-based sensors, the DPS system provides high spatial resolution data, enabling the detection of localized phenomena - such as preferential flow paths or, as observed in the test embankment, changes in permeability due to variations in soil materials or their properties - that may be overlooked by discrete sensors.

DPS systems offer significant advantages over traditional point-based instrumentation, particularly in terms of spatial resolution and potential cost efficiency. Although the initial cost of interrogation units is relatively high, the ability to continuously monitor pore pressure along the full length of the cable reduces the need for multiple point sensors. In terms of coverage efficiency, an approximate ratio of 1:10 can be considered - meaning that for every point sensor replaced, approximately 10 meters of DPS cable can be installed, providing continuous data across that distance. This estimate does not yet account for further cost savings from reduced installation time, simplified cabling, and fewer data loggers or interrogation devices.

Overall, DPS systems show strong potential to provide substantial technical and logistical benefits, especially in large-scale or long-term geotechnical and hydraulic monitoring applications. However, to further validate the long-term reliability of the DPS technology, future work should include extended monitoring campaigns to assess sensor drift, determine optimal calibration intervals, and develop standardized maintenance protocols. Although the DPS technology has not yet been extensively tested, several research projects are planned to explore its deployment in various environmental and structural settings, aiming to broaden its validation across different use cases, such as:

 Application of DPS for detecting and monitoring backward erosion piping within the framework of the LIFE SandBoil project [18];

- Implementation of the DPS system in a real river dike section of the Rhone dike in the Canton of Valais, (Switzerland) [9].
- Large-scale testing of DPS for dynamic wave measurement, expanding upon previous work introduced by Höttges, et al. [19]

These developments are expected to contribute significantly to the broader adoption of distributed sensing technologies in hydraulic and geotechnical engineering.

ACKNOWLEDGMENTS

The authors would like to thank the financial supporters of this project: the Swiss Federal Institute for the Environment (FOEN) and the Cantonal Service for Flood Protection of the 3rd Rhone.

Special thanks go to the team at the University of Applied Sciences in Rapperswil (OST), particularly Isabel Bohren for designing the test embankment and assisting with sensor installation, and Dr. Antonio Salazar for his help with data analysis and processing.

We are also grateful to the AIPo team – especially Agnese Bassi, Giuseppe Capuano and Luca Crose - for their support during the embankment construction and sensor installation. Thanks to Idrovie Ltd. construction company for their dedication during the work.

The authors also wish to thank SISGEO Ltd. for their support during the installation of the conventional monitoring system, especially Daniel Naterop and Vincenzo Caci.

We further acknowledge the geotechnical group at the University of Bologna, with thanks to Prof. Dr. Guido Gottardi, Dr. Michela Marchi, and Dr. Ilaria Bertolini for their support and expertise during the design of the embankment and the sensor installation. Appreciation is also extended to the geotechnical group at the University of Padova of Prof. Dr. Simonetta Cola, particularly Dr. Nicola Fabbian, for his assistance with the sensor installation and the design of the measuring system.

Finally, sincere thanks to Dr. Massimo Facchini for his assistance during the measurement campaign and his contribution to the design of the DFO measuring system.

REFERENCES

- [1] L. Cremonini, P. Randi, M. Fazzini, M. Nardino, F. Rossi, and T. Georgiadis, "Causes and Impacts of Flood Events in Emilia-Romagna (Italy) in May 2023," *Land*, vol. 13, no. 11, p. 1800, 2024. [Online]. Available: https://www.mdpi.com/2073-445X/13/11/1800.
- [2] D. Zumofen, "Flooding of the Rhone in Switzerland on 29/30 June 2024: Problems, immediate measures and projects.," in 30th Meeting of the European Working Group on Internal Erosion in Embankment Dams, Dikes and Levees and their Foundations, Bologna, 2024.
- [3] M. Foster, R. Fell, and M. Spannagle, "The statistics of embankment dam failures and accidents," *Canadian Geotechnical Journal*, vol. 37, no. 5, pp. 1000-1024, 2000.
- [4] R. Fell, C. F. Wan, J. Cyganiewicz, and M. Foster, "Time for development of internal erosion and piping in embankment dams," (in English), *Journal of Geotechnical and Geoenvironmental Engineering*, vol. 129, no. 4, pp. 307-314, Apr 2003.
- [5] L. Schenato, "A Review of Distributed Fibre Optic Sensors for Geo-Hydrological Applications," (in English), Applied Sciences-Basel, vol. 7, no. 9, Sep 2017.
- [6] N. Fabbian, P. Simonini, F. De Polo, L. Schenato, and S. Cola, "Temperature monitoring in levees for detection of seepage,"



- Bulletin of Engineering Geology and the Environment, vol. 83, no. 2, pp. 1-12, 2024.
- [7] A. Höttges, C. Rabaiotti, and M. Facchini, "A novel distributed fiber optic hydrostatic pressure sensor for dike safety monitoring," *IEEE Sensors Journal*, vol. 23, no. 23, pp. 28942-28953, 2023, doi: 10.1109/JSEN.2023.3315062.
- [8] A. Höttges, C. Rabaiotti, and M. Facchini, "A ground-breaking Distributed fiber-optic Pressure Sensor for geohydraulic applications," *Procedia Structural Integrity*, vol. 64, pp. 1613-1620, 2024/01/01/ 2024, doi: https://doi.org/10.1016/j.prostr.2024.09.416.
- [9] C. Rabaiotti, A. Höttges, M. Facchini, and I. Bohren, "FIBRADIKE, a novel distributed fiber optic monitoring system for dikes and earth dams," in *IOP Conference Series: Earth and Environmental Science*, 2023, vol. 1195, no. 1: IOP Publishing, p. 012004
- [10] M. Froggatt and J. Moore, "High-spatial-resolution distributed strain measurement in optical fiber with Rayleigh scatter," *Applied optics*, vol. 37, no. 10, pp. 1735-1740, 1998.
- [11] E. N. Allouche, S. T. Ariaratnam, and J. S. Lueke, "Horizontal directional drilling: Profile of an emerging industry," *Journal of Construction Engineering and Management*, vol. 126, no. 1, pp. 68-76, 2000
- [12] LUNA, "OBR 4600 Data Sheet," ed: Luna Innovations Incorporate, 2025.
- [13] APSensing, "DTS N45-Series Data Sheet," ed: AP Sensing 2025.
- [14] N. Coca-Lopez, "An intuitive approach for spike removal in Raman spectra based on peaks' prominence and width," *Analytica Chimica Acta*, 2024.
- [15] A. Savitzky and M. J. Golay, "Smoothing and differentiation of data by simplified least squares procedures," *Analytical chemistry*, vol. 36, no. 8, pp. 1627-1639, 1964.
- [16] K. Terzaghi, R. B. Peck, and G. Mesri, Soil mechanics in engineering practice. John wiley & sons, 1996.
- [17] M. W. Bo and J. Barrett, "Types of instruments," in *Geotechnical Instrumentation and Applications*: Springer, 2023, pp. 31-72.
- [18] L. Tonni, M. Marchi, A. Bassi, and A. Rosso, "A Sand Boil Database for Piping Risk Management in the Po River, Italy," *Water*, vol. 16, no. 10, p. 1384, 2024. [Online]. Available: https://www.mdpi.com/2073-4441/16/10/1384.
- [19] A. Höttges, M. Smaadahl, F. M. Evers, R. M. Boes, and C. Rabaiotti, "Dynamic wave measurement with a high spatial resolution distributed fiber optic pressure sensor," *IEEE Sensors Journal*, vol. 24, no. 14, pp. 22387-22396, 2024, doi: 10.1109/JSEN.2024.3401414.